HAL
open science

On the Behavior of Upwind Schemes in the Low Mach Number Limit

Hervé Guillard, Cécile Viozat

To cite this version:

Hervé Guillard, Cécile Viozat. On the Behavior of Upwind Schemes in the Low Mach Number Limit. RR-3160, INRIA. 1997. inria-00073529

HAL Id: inria-00073529

https://inria.hal.science/inria-00073529v1

Submitted on 24 May 2006

HAL is a multi-disciplinary open access archive for the deposit and dissemination of scientific research documents, whether they are published or not. The documents may come from teaching and research institutions in France or abroad, or from public or private research centers.

L'archive ouverte pluridisciplinaire **HAL**, est destinée au dépôt et à la diffusion de documents scientifiques de niveau recherche, publiés ou non, émanant des établissements d'enseignement et de recherche français ou étrangers, des laboratoires publics ou privés.

INSTITUT NATIONAL DE RECHERCHE EN INFORMATIQUE ET EN AUTOMATIQUE

On the Behavior of Upwind Schemes in the Low Mach Number Limit

Hervé Guillard , Cécile Viozat

N° 3160

Avril 1997

THÈME 4

Rapport de recherche

ISSN 0249-6399

On the Behavior of Upwind Schemes in the Low Mach Number Limit

Hervé Guillard *, Cécile Viozat **

Thème 4 — Simulation et optimisation
de systèmes complexes
Projet SINUS

Rapport de recherche n ° 3160 — Avril 1997 — 28 pages

Abstract: This paper presents an asymptotic analysis in power of the Mach number of the flux difference splitting approximation of the compressible Euler equations in the low Mach number limit. We prove that the solutions of the discrete system contain pressure fluctuations of order Ma while the continuous pressure scales with the square of the Mach number. This explains in a rigorous manner why this approximation of the compressible equations fails to compute very subsonic flow. We then show that a preconditioning of the numerical dissipation tensor allows to recover a correct scaling of the pressure. These theoretical results are totally confirmed by numerical experiments.

Key-words: Low Mach number, flux difference splitting upwind schemes, Roe scheme, preconditioning

(Résumé : tsvp)

* E-mail:Herve.Guillard@sophia.inria.fr
** E-mail:Cecile.Viozat@sophia.inria.fr

Unité de recherche INRIA Sophia Antipolis
2004 route des Lucioles, BP 93, 06902 SOPHIA ANTIPOLIS Cedex (France)
Téléphone : 04 93 65 77 77 – Télécopie : 04 93 65 77 65

Sur le comportement des schémas décentrés à la limite petit nombre de Mach

Résumé : Ce papier présente une analyse asymptotique en terme du nombre de Mach de l'approximation par décomposition de différence de flux des équations d'Euler pour un fluide compressible à la limite petit nombre de Mach. Nous prouvons que les solutions du système discret contiennent des fluctuations de pressions de l'ordre du nombre de Mach alors que celles du système continu contiennent des fluctuations de pressions de l'ordre du nombre de Mach au carré. Ceci explique de manière rigoureuse pourquoi cette approximation des équations pour les fluides compressibles ne permet pas de calculer des écoulements très subsoniques. Nous montrons ensuite qu'un préconditionnement du tenseur de la dissipation numérique permet de retrouver un ordre de grandeur correct de la pression. Ces résultats théoriques sont totalement confirmés par les expériences numériques.

Mots-clé : Petit nombre de Mach, schémas décentrés, schéma de Roe, préconditionnement

Contents

1 Introduction **1**

2 The continuous case **2**

3 The discrete case **6**

4 Preconditioned dissipation **14**

5 Conclusion **23**

6 Acknowledgments **24**

1 Introduction

It is well-known that in addition to convergence and round-off difficulties, the upwind approximations of the compressible fluid flow equations suffer from accuracy problems in the Low-Mach number limit. There are experimental evidences showing that on a fixed mesh, the discretized solution of the compressible fluid flow equations are not an accurate approximation of the incompressible equations (e.g see [9] [4]).
A common explanation of this failure of compressible upwind schemes is to put forward the role of the numerical dissipation. In upwind schemes, the numerical dissipation associated with the two grid nodes $\boldsymbol{i}$ and $\boldsymbol{l}$ is of the form :

$$\delta|A|\Delta_{\boldsymbol{il}}q = \delta\sum_i |\lambda_i|\alpha_i(\Delta_{\boldsymbol{il}})R_i \tag{1}$$

where δ is the mesh size, λ_i and R_i are respectively the eigenvalues and eigenvectors of the jacobian matrix A, $\alpha_i(\Delta_{\boldsymbol{il}})$ are the coordinate of the jump $\Delta_{\boldsymbol{il}}q$ between the values of the function at the grid nodes $\boldsymbol{i}$ and $\boldsymbol{l}$ in the basis formed by the eigenvectors. In the above expression, the sum runs over all waves. If we introduce a reference Mach number M_* we see that this implies that some of the wave speeds λ_i become proportional to $1/M_*$. Thus in the low Mach number limit these terms can grow without bound resulting in an excessive numerical dissipation that pollutes the discrete solution.

We believe that this explanation is only partially true and needs to be refined. First we remark that, if the dissipative terms are of order $1/M_*$, the centered terms in the approximation scale with $1/M_*^2$ (see section 2). Thus although the amplitude of the dissipative terms may go to infinity, they become negligible with respect to the centered ones as M_* goes to zero. Therefore, the accuracy problem may actually result from a lack of numerical dissipation instead of resulting from an excess of numerical viscosity. Second, in upwind schemes, the numerical dissipation is a 4×4 tensor (in 2-D) and although some of the λ_i goes to infinity, it may well be that the discrete equations force the associated jumps $\alpha_i(\Delta_{\boldsymbol{il}})$ to go to zero.

Our aim in this work is thus to explain in a detailed manner the mechanism by which compressible upwind schemes fail to compute very subsonic flows. The tool we will use for this study, is only a standard asymptotic analysis in power of the Mach number. However, this analysis will be performed on the *discrete equations* instead of the continuous ones. More specifically, we will look for the asymptotic form that takes the discrete system in the low Mach number limit. The analysis we performed is a fully non-linear one that does not require any linearization of the governing equations. Moreover, it applies to the steady state equations as well as the time dependent ones. Its main result can be stated as follows :
In the low Mach number limit, the solution of the *discrete equations* contains pressure fluctuations of order Mach.
This is in clear contrast with the continuous case where pressure fluctuations scale with the

square of the Mach number.

For the steady state equations, a common strategy to overcome the convergence problems encountered by compressible solvers is the use of *preconditioning* [5, 6, 7, 3]. Following a suggestion in [7] we tried in [8] to use preconditioning as a cure to the accuracy problem. The results were extremely convincing and it appears that preconditioning is a powerful remedy to cure the accuracy problem. More specifically, the dissipative term in (1) $\delta|A|\Delta q$ is changed into :

$$\delta P^{-1}|PA|\Delta q \tag{2}$$

where P is the preconditioning matrix. However *the temporal and centered terms of the approximation remain unchanged (i.e with no preconditioning).* Therefore, the scheme is always consistent with the time-dependent equations and only the numerical dissipation is altered. Although more complex than in the case with no preconditioning, an asymptotic analysis of the resulting discrete equations appears to be tractable. It provides a detailed explanation of the mechanism by which preconditioning increases the accuracy of the schemes. In particular, it shows that preconditioning *increases* the numerical dissipation terms associated to the continuity and energy equations by a factor $1/M_*$. Thus, contrarily to the non-preconditioned case, the non-dimensional discrete equations contain no term of order $1/M_*$ as in the continuous case. Solving these equations gives pressure that possesses the same M_*^2 scaling as for the continuous system.

The analysis presented in this work uses Roe's approximate Riemann solver. This scheme possesses some nice algebraic features that simplify to some extent the discrete equations. However, the analysis is general and applies to all the schemes that can be cast under the form (1) with a matrix A that is the Jacobian of the continuous fluxes evaluated at some average between $\boldsymbol{i}$ and $\boldsymbol{l}$. The outline of this paper is as follows : In the next section, we recall how to derive the convergence of the compressible Euler equations toward the incompressible ones. Next, we apply the same asymptotic expansions as in the continuous case to the discrete Roe scheme and finally, in the last section, we examine the case of a preconditioned dissipation.

2 The continuous case

The equations of motion of inviscid compressible fluids write :

$$\frac{\partial}{\partial t}\rho \quad + div(\rho\vec{u}) \qquad\qquad = 0 \qquad (3.a)$$

$$\frac{\partial}{\partial t}\rho\vec{u} \quad + div(\rho\vec{u}\otimes\vec{u}) \quad + \nabla p \quad = 0 \qquad (3.b)$$

$$\frac{\partial}{\partial t}\rho e \quad + div(\rho e\vec{u} \qquad + p\vec{u}) \quad = 0 \qquad (3.c)$$

where ρ is the fluid density, $\vec{u}$ the velocity and e the total energy defined as the sum of the internal energy plus the kinetic energy.

$$e = C_v T + \frac{1}{2}(u^2 + v^2 + w^2) \tag{4}$$

p is the pressure defined as $p = \rho RT$ where R is the perfect gas constant and T the temperature. Equation (4) and the perfect gas law can be combined to yield :

$$p = (\gamma - 1)(\rho e - \frac{1}{2}\rho(u^2 + v^2 + w^2)) \tag{5}$$

On the other hand, the incompressible Euler equations are :

$$div(\vec{u}) = 0 \qquad (6.a)$$

$$\rho_0(\frac{\partial}{\partial t}\vec{u} \quad + div(\vec{u}\otimes\vec{u})) \quad + \nabla\pi \quad = 0 \qquad (6.b)$$

where ρ_0 is a constant reference density and π the dynamic pressure. The incompressible fluid equations are known to be the singular limit of the compressible Euler equations when $Ma \to 0$. As an introduction to the computations that will be carried out in section 3, we recall here how to formally derive this singular limit. The first step of this derivation is performed through the nondimensionalization of the compressible Euler equations. Let $\rho_i(x)$, $\vec{u}_i(x)$ and $p_i(x)$ be the initial values of the density, velocity and pressure fields. Let $\rho^* = \max_x(\rho_i(x))$, $u^* = \max_x(|\vec{u}_i(x)|)$ and let the sound speed scale a^* be defined by :

$\rho^*(a^*)^2 = \gamma max_x(p_i(x))$. Introducing the new non-dimensionalized variables :

$$\begin{aligned} \tilde{\rho} &= \frac{\rho}{\rho^*}, \qquad \tilde{u} = \frac{\vec{u}}{u^*}, \quad \tilde{p} = \frac{p}{\rho^*(a^*)^2} \\ \tilde{e} &= \frac{e}{(a^*)^2}, \quad \tilde{x} = \frac{x}{\delta^*}, \quad \tilde{t} = \frac{tu^*}{\delta^*} \end{aligned} \tag{7}$$

where δ^* is an arbitrary length scale, we obtain the system of non-dimensionalized equations :

$$\frac{\partial}{\partial \tilde{t}}\tilde{\rho} \quad + div(\tilde{\rho}\tilde{u}) \quad = 0 \qquad (8.a)$$

$$\frac{\partial}{\partial \tilde{t}}\tilde{\rho}\tilde{u} \quad + div(\tilde{\rho}\tilde{u} \otimes \tilde{u}) \quad + \frac{1}{M_*^2}\nabla\tilde{p} \quad = 0 \qquad (8.b)$$

$$\frac{\partial}{\partial \tilde{t}}\tilde{\rho}\tilde{e} \quad + div(\tilde{\rho}\tilde{e}\tilde{u} \quad + \tilde{p}\tilde{u}) \quad = 0 \qquad (8.c)$$

where $M_* = u^*/a^*$ is the reference Mach number. The non-dimensionalized state law (5) takes the form :

$$\tilde{p} = (\gamma - 1)(\tilde{\rho}\tilde{e} - \frac{M_*^2}{2}\tilde{\rho}(\tilde{u}^2 + \tilde{v}^2 + \tilde{w}^2)) \tag{9}$$

We now look for solutions of the system (8) in the form of asymptotic expansion in power of the Mach number :

$$\begin{aligned} \tilde{\rho} &= \tilde{\rho}_0 + M_*\tilde{\rho}_1 + M_*^2\tilde{\rho}_2 + \dots \\ \tilde{u} &= \tilde{u}_0 + M_*\tilde{u}_1 + M_*^2\tilde{u}_2 + \dots \\ \tilde{p} &= \tilde{p}_0 + M_*\tilde{p}_1 + M_*^2\tilde{p}_2 + \dots \\ \tilde{e} &= \tilde{e}_0 + M_*\tilde{e}_1 + M_*^2\tilde{e}_2 + \dots \\ \dots &= \dots \end{aligned}$$

Introducing these expressions in the equations (8) and collecting the terms with equal power of M_* we obtain (we have dropped the ˜ for convenience):

1. Order $1/M_*^2$

$$\nabla p_0 = 0 \tag{10}$$

2. Order $1/M_*$

$$\nabla p_1 = 0 \tag{11}$$

3. Order 0

$$\begin{aligned}
\frac{\partial}{\partial t}\rho_0 \quad &+ div(\rho_0 u_0) && = 0 && (12.a)\\
\frac{\partial}{\partial t}\rho_0 u_0 \quad &+ div(\rho_0 u_0 \otimes u_0) \quad + \nabla p_2 && = 0 && (12.b)\\
\frac{\partial}{\partial t}\rho_0 e_0 \quad &+ div(\rho_0 e_0 u_0 \quad + p_0 u_0) && = 0 && (12.c)
\end{aligned}$$

while the 0-order state law becomes :

$$p_0 = (\gamma - 1)(\rho_0 e_0)$$

The order $1/M_*^2$ and $1/M_*$ equations imply that the pressure is constant in space up to fluctuations of order M_*^2. Thus we may write :

$$p(x,t) = P_0(t) + M_*^2 p_2(x,t)$$

In the presence of open boundaries, the thermodynamic pressure P_0 will be equal to the exterior pressure that we assume for simplicity constant in time :

$$\frac{dP_{ext}}{dt} = \frac{dP_0}{dt} = 0$$

We deduce from the non-dimensionalized 0-order state law that $\frac{\partial \rho_0 e_0}{\partial t} = \nabla \rho_0 e_0 = 0$ and the energy equation (12.c) degenerates into :

$$div u_0 = 0$$

Introducing this relation into the continuity equation, we see that this implies that the material derivative of the density is zero. Assuming for simplicity that all particle paths come from regions with the same density, we conclude that :

$$\rho_0 = Cte$$

and that the 0-order system reduces to the following set of equations [1] :

$$\rho_0 = Cte \tag{13.a}$$

$$\rho_0(\frac{\partial}{\partial t}u_0 \quad div(u_0 \otimes u_0)) \quad + \nabla p_2 \quad = 0 \tag{13.b}$$

$$div(u_0) = 0 \tag{13.c}$$

3 The discrete case

Our aim is now to perform a similar analysis of the low Mach number behavior of the *discrete* compressible Euler equations when a flux difference upwind method is used to approximate system (3). For simplicity, we consider that we use a regular cartesian grid of uniform mesh size δ in two dimensions. $\boldsymbol{i} = (i, j)$ is the index of the node whose coordinates are $(i\delta, j\delta)$ and we use the notation $\mathcal{V}(\boldsymbol{i}) = \{(i-1, j), (i+1, j), (i, j-1), (i, j+1)\}$ or $\mathcal{V}(\boldsymbol{i}) = \{N, S, E, W\}$ for labelling the neighbors of the grid node $\boldsymbol{i}$. The cell associated with node $\boldsymbol{i}$ is $C_{\boldsymbol{i}} = [(i-1/2)\delta, (i+1/2)\delta] \times [(j-1/2)\delta, (j+1/2)\delta]$, $\vec{n}$ is the outward unit normal vector on $\partial C_{\boldsymbol{i}}$ and we note $\vec{n}_{\boldsymbol{il}} = \dfrac{\int_{C_{\boldsymbol{i}} \cap C_{\boldsymbol{l}}} \vec{n}}{\delta}$.

The application of Roe's approximate Riemann solver in a first-order finite volume scheme yields the following set of semi-discrete equations (see appendix I. for details) :

[1] Here, we have derived the singular limit of the compressible Euler equations using the conservative energy equation and the perfect gas state law. In the low Mach number limit, one can safely assume that no shock waves are present, consequently the energy equation and the state law can be replaced by $p/\rho^\gamma =$ constant. In this case, the incompressible limit can be obtained from the isentropic compressible equations in essentially the same way, for a rigorous (not formal) proof see [1]. Here, we prefer to use the complete non isentropic compressible system to point out the differences with the discretized equations

$$\delta\frac{\partial}{\partial t}\rho_i \quad +\frac{1}{2}\sum_{l\in\mathcal{V}(i)}\rho_l\vec{u}_l.\vec{n}_{il}$$

$$+\frac{1}{2}\sum_{l\in\mathcal{V}(i)}|U_{il}|(\Delta_{il}\rho-\frac{\Delta_{il}p}{a_{il}^2})+\rho_{il}\frac{U_{il}}{a_{il}}\Delta_{il}U+\frac{\Delta_{il}p}{a_{il}}=0 \qquad (14.a)$$

$$\delta\frac{\partial}{\partial t}\rho_i u_i \quad +\frac{1}{2}\sum_{l\in\mathcal{V}(i)}\rho_l u_l\vec{u}_l.\vec{n}_{il}+p_l(n_x)_{il}$$

$$+\frac{1}{2}\sum_{l\in\mathcal{V}(i)}|U_{il}|(\Delta_{il}\rho-\frac{\Delta_{il}p}{a_{il}^2})u_{il}+\rho_{il}\frac{U_{il}}{a_{il}}u_{il}\Delta_{il}U$$

$$-\rho_{il}|U_{il}|(n_y)_{il}\Delta_{il}V+\frac{(Un_x+u)_{il}}{a_{il}}\Delta_{il}p+\rho_{il}a_{il}(n_x)_{il}\Delta_{il}U=0 \qquad (14.b)$$

$$\delta\frac{\partial}{\partial t}\rho_i v_i \quad +\frac{1}{2}\sum_{l\in\mathcal{V}(i)}\rho_l v_l\vec{u}_l.\vec{n}_{il}+p_l(n_y)_{il}$$

$$+\frac{1}{2}\sum_{l\in\mathcal{V}(i)}|U_{il}|(\Delta_{il}\rho-\frac{\Delta_{il}p}{a_{il}^2})v_{il}+\rho_{il}\frac{U_{il}}{a_{il}}v_{il}\Delta_{il}U$$

$$+\rho_{il}|U_{il}|(n_x)_{il}\Delta_{il}V+\frac{(Un_y+v)_{il}}{a_{il}}\Delta_{il}p+\rho_{il}a_{il}(n_y)_{il}\Delta_{il}U=0 \qquad (14.c)$$

$$\delta\frac{\partial}{\partial t}\rho_i e_i \quad +\frac{1}{2}\sum_{l\in\mathcal{V}(i)}(\rho_l e_l+p_l)\vec{u}_l.\vec{n}_{il}$$

$$+\frac{1}{2}\sum_{l\in\mathcal{V}(i)}|U_{il}|(\Delta_{il}\rho-\frac{\Delta_{il}p}{a_{il}^2})(\frac{u_{il}^2+v_{il}^2}{2})+\rho_{il}\frac{U_{il}}{a_{il}}h_{il}\Delta_{il}U$$

$$+\rho_{il}|U_{il}|V_{il}\Delta_{il}V+\frac{(h+U^2)_{il}}{a_{il}}\Delta_{il}p+\rho_{il}a_{il}U_{il}\Delta_{il}U=0 \qquad (14.d)$$

---

where we have introduced the additional notations :

$$\Delta_{il}(.)=(.)_i-(.)_l;\;\; U=\vec{u}.\vec{n};\;\; V=-un_y+vn_x$$

$$\rho_{il} = \sqrt{\rho_i \rho_l}$$

$(h, u, v)_{il}$ denotes the Roe average between the states $(h, u, v)_i$ and $(h, u, v)_l$ defined by :

$$h_{il} = \frac{h_i\sqrt{\rho_i} + h_l\sqrt{\rho_l}}{\sqrt{\rho_i} + \sqrt{\rho_l}}; \ (u, v)_{il} = \frac{(u, v)_i\sqrt{\rho_i} + (u, v)_l\sqrt{\rho_l}}{\sqrt{\rho_i} + \sqrt{\rho_l}}$$

with h the specific enthalpy given by :

$$h = e + \frac{p}{\rho}$$

The average sound speed a_{il} is given by :

$$a_{il}^2 = (\gamma - 1)\left(h_{il} - \frac{1}{2}(u_{il}^2 + v_{il}^2)\right)$$

Using now the same dimensionless variables as in section 2 (see equations (7)) we obtain from system (14):

$$\frac{1}{2M_*}\sum_{l\in\mathcal{V}(i)}\frac{\Delta_{il}p}{a_{il}}+$$
$$\tilde{\delta}\frac{d}{dt}\rho_i+\frac{1}{2}\sum_{l\in\mathcal{V}(i)}\rho_l\vec{u}_l.\vec{n}_{il}+|U_{il}|(\Delta_{il}\rho-\frac{\Delta_{il}p}{a_{il}^2})+$$
$$\frac{M_*}{2}\sum_{l\in\mathcal{V}(i)}\rho_{il}\frac{U_{il}}{a_{il}}\Delta_{il}U=0 \qquad (15.a)$$

$$\frac{1}{2M_*^2}\sum_{l\in\mathcal{V}(i)}p_l(n_x)_{il}+$$
$$\frac{1}{2M_*}\sum_{l\in\mathcal{V}(i)}\frac{(Un_x+u)_{il}}{a_{il}}\Delta_{il}p+\rho_{il}a_{il}(n_x)_{il}\Delta_{il}U+$$
$$\tilde{\delta}\frac{d}{dt}\rho_i u_i+\frac{1}{2}\sum_{l\in\mathcal{V}(i)}\rho_l u_l\vec{u}_l.\vec{n}_{il}+|U_{il}|(\Delta_{il}\rho-\frac{\Delta_{il}p}{a_{il}^2})u_{il}-\rho_{il}|U_{il}|(n_y)_{il}\Delta_{il}V+$$
$$\frac{M_*}{2}\sum_{l\in\mathcal{V}(i)}\rho_{il}\frac{U_{il}}{a_{il}}u_{il}\Delta_{il}U=0 \qquad (15.b)$$

$$\frac{1}{2M_*^2}\sum_{l\in\mathcal{V}(i)}p_l(n_y)_{il}+$$
$$\frac{1}{2M_*}\sum_{l\in\mathcal{V}(i)}\frac{(Un_y+v)_{il}}{a_{il}}\Delta_{il}p+\rho_{il}a_{il}(n_y)_{il}\Delta_{il}U+$$
$$\tilde{\delta}\frac{d}{dt}\rho_i v_i+\frac{1}{2}\sum_{l\in\mathcal{V}(i)}\rho_l v_l\vec{u}_l.\vec{n}_{il}+|U_{il}|(\Delta_{il}\rho-\frac{\Delta_{il}p}{a_{il}^2})v_{il}+\rho_{il}|U_{il}|(n_x)_{il}\Delta_{il}V+$$
$$\frac{M_*}{2}\sum_{l\in\mathcal{V}(i)}\rho_{il}\frac{U_{il}}{a_{il}}v_{il}\Delta_{il}U=0 \qquad (15.c)$$

$$\frac{1}{2M_*}\sum_{l\in\mathcal{V}(i)}\frac{h_{il}}{a_{il}}\Delta_{il}p+$$
$$\tilde{\delta}\frac{d}{dt}\rho_i e_i+\frac{1}{2}\sum_{l\in\mathcal{V}(i)}(\rho_l e_l+p_l)\vec{u}_l.\vec{n}_{il}+$$
$$\frac{M_*}{2}\sum_{l\in\mathcal{V}(i)}\frac{U_{il}^2}{a_{il}}\Delta_{il}p+\rho_{il}a_{il}U_{il}\Delta_{il}U+\rho_{il}\frac{U_{il}}{a_{il}}h_{il}\Delta_{il}U+$$
$$\frac{M_*^2}{2}\sum_{l\in\mathcal{V}(i)}|U_{il}|(\Delta_{il}\rho-\frac{\Delta_{il}p}{a_{il}^2})(\frac{u_{il}^2+v_{il}^2}{2})+\rho_{il}|U_{il}|V_{il}\Delta_{il}V=0 \qquad (15.d)$$

while the dimensionless equation of state is given by (9).

Following the method used in the continuous case, we next expand all the variables in power of the reference Mach number M_* :

$$(.) = (.)_0 + M_*(.)_1 + M_*^2(.)_2 + \dots \tag{16}$$

and introduce these expansions into system (15). Collecting terms with equal power of M_*, we obtain :

1. Order $1/M_*^2$

$$p_N^0 - p_S^0 = 0; \quad p_E^0 - p_W^0 = 0 \tag{17}$$

2. Order $1/M_*$

   (a) Continuity equation

$$\frac{1}{2}\sum_{\boldsymbol{l}\in\mathcal{V}(\boldsymbol{i})} \frac{\Delta_{\boldsymbol{il}} p^0}{a^0_{\boldsymbol{il}}} = 0 \tag{18}$$

   (b) horizontal momentum equation

$$\frac{1}{2}\sum_{\boldsymbol{l}\in\mathcal{V}(\boldsymbol{i})} \frac{(U^0 n_x + u^0)_{\boldsymbol{il}}}{a^0_{\boldsymbol{il}}} \Delta_{\boldsymbol{il}} p^0 + \rho^0_{\boldsymbol{il}} a^0_{\boldsymbol{il}} (n_x)_{\boldsymbol{il}} \Delta_{\boldsymbol{il}} U^0 + \sum_{\boldsymbol{l}\in\mathcal{V}(\boldsymbol{i})} p^1_{\boldsymbol{l}} (n_x)_{\boldsymbol{il}} = 0 \tag{19}$$

   (c) vertical momentum equation

$$\frac{1}{2}\sum_{\boldsymbol{l}\in\mathcal{V}(\boldsymbol{i})} \frac{(U^0 n_y + v^0)_{\boldsymbol{il}}}{a^0_{\boldsymbol{il}}} \Delta_{\boldsymbol{il}} p^0 + \rho^0_{\boldsymbol{il}} a^0_{\boldsymbol{il}} (n_y)_{\boldsymbol{il}} \Delta_{\boldsymbol{il}} U^0 + \sum_{\boldsymbol{l}\in\mathcal{V}(\boldsymbol{i})} p^1_{\boldsymbol{l}} (n_y)_{\boldsymbol{il}} = 0 \tag{20}$$

   (d) energy equation

$$\frac{1}{2}\sum_{\boldsymbol{l}\in\mathcal{V}(\boldsymbol{i})} \frac{h^0_{\boldsymbol{il}}}{a^0_{\boldsymbol{il}}} \Delta_{\boldsymbol{il}} p^0 = 0 \tag{21}$$

Now, let us solve (17)-(18)-(19) (20)-(21), we have :

Lemma 3.1 *(17) and (18) (or (17) and (21)) imply that* $p^0_{\boldsymbol{l}} = cte \ \forall \boldsymbol{l}$.

Proof : (17) implies that p^0 has a four field solution of the form depicted in figure 1 :

B	**A**	**B**	**A**	**B**	**A**	
D	**C**	**D**	**C**	**D**	**C**	
B	**A**	**B**	**A**	**B**	**A**	
D	**C**	**D**	**C**	**D**	**C**	

Figure 1: Four field solution of the $1/M_*^2$ order equation (17)

To prove that the spurious pressure mode $p^0_{i,l} = A, p^0_{i+1,l} = B, p^0_{i,l+1} = C, p^0_{i+1,l+1} = D$ is not actually present in the solution, assume for instance that A is the maximum of the four value A, B, C, D. We note now that the coefficients of (18) are positive. Thus all the terms in the sum (18) are positive and (18) cannot equal 0 unless $A = B = C = D$. In other words, the discrete maximum principle applies and necessarily the four values in the set A, B, C, D are equal.

Therefore we see that the $1/M_*$-order momentum equations (19) - (20) reduce to :

$$p^1_E - p^1_W = \rho^0_{\boldsymbol{i}_E} a^0_{\boldsymbol{i}_E} \Delta_{\boldsymbol{i}_E} U^0 + \rho^0_{\boldsymbol{i}_W} a^0_{\boldsymbol{i}_W} \Delta_{\boldsymbol{i}_W} U^0 \tag{22}$$

and

$$p^1_N - p^1_S = \rho^0_{\boldsymbol{i}_N} a^0_{\boldsymbol{i}_N} \Delta_{\boldsymbol{i}_N} U^0 + \rho^0_{\boldsymbol{i}_S} a^0_{\boldsymbol{i}_S} \Delta_{\boldsymbol{i}_S} U^0 \tag{23}$$

These equations *do* imply that the order M_* pressure p^1 is *not* a constant. Thus we have :

Proposition 3.1 *The solutions of the discrete Euler equations (14) support pressure fluctuations of order* M_* *:*

$$p(x,t) = P_0(t) + M_* p_1(x,t) \tag{24}$$

This is in clear contrast with the continuous case where pressure fluctuations scale as M_*^2.

Therefore, on a *fixed mesh* (δ = constant), we cannot recover the correct scaling of the pressure with the Mach number. The discrete solutions of equation (14) exhibit pressure fluctuations that are much larger than in the continuous case. Moreover the ratio between the numerical pressure fluctuations and the exact ones will increase as the Mach number goes to zero.

In order to illustrate the above theory, we consider a sequence of computations of the flow around a NACA0012 airflow at decreasing Mach number on the same *fixed* mesh. Figure 2 shows the pressure fields obtained for three different inflow Mach numbers. In these computations, the inflow velocity is kept constant equal to unity while the inflow pressure is increased. To allow a comparison between the pressure fields at different Mach number, Figure 2 shows the normalized pressure p_{norm} defined as $p_{norm} = p - p_{\min}/p_{\max} - p_{\min}$. As the Mach number decreases, the results become worse and the solutions do not converge to a reasonnable approximation of the incompressible solution. Actually, the $Mach = 0.1$ solution is closer to the incompressible one than is the $Mach = 0.001$ solution. This point was already noticed (e.g [9]) by several other investigators.

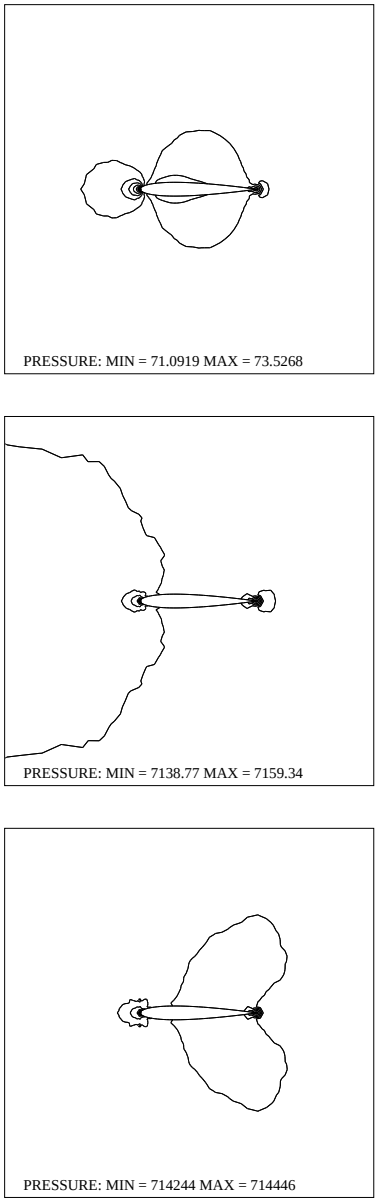

Figure 2: Isovalues of the pressure, on a 3114 node mesh for $M_\infty = 0.1$ (top), $M_\infty = 0.01$ (middle), $M_\infty = 0.001$ (bottom).

Figure 3 that displays the pressure fluctuation $(P_{\max} - P_{\min})/P_{\max}$ versus the inflow Mach number, explains why this behavior occurs. In perfect agreement with the theoretical predictions, it is easily checked that the pressure fluctuations are proportional to the Mach number. Thus the accuracy of the numerical results in the incompressible limit is very low and this accuracy deteriorates as the Mach number decreases.

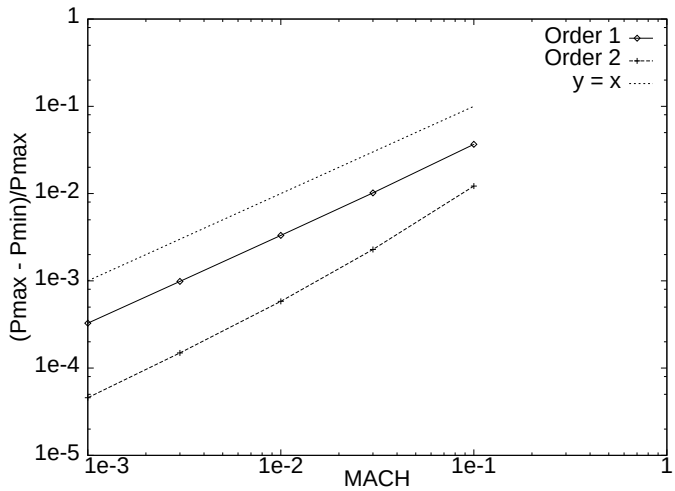

Figure 3: Pressure fluctuations versus inflow Mach number; solid line : order 1, dashed line : order 2. For comparison, the curve y=x is represented by a dotted line.

One way to recover a better accuracy could be to use an improved spatial approximation. On figure 3 is also plotted the results obtained with a second order MUSCL type scheme. Although, the previous theory does not strictly apply to this case where the dissipative terms are of fourth order while the theory has been performed for second order dissipative terms, it can be seen that the pressure fluctuations still scale approximately with the Mach number and not with its square. Therefore the use of second order schemes gives only a marginal improvement with respect to the first order ones.

4 Preconditioned dissipation

In this section, we performed a similar study in the case where Roe's dissipation is modified by preconditioning. Specifically, let $A(q_{il})$ be the Roe matrix associated to nodes i and l, we change the numerical flux into :

$$\Phi(q_i, q_l, \vec{n}_{il}) = \frac{\vec{F}(q_i) + \vec{F}(q_l)}{2} \cdot \vec{n_{il}} + \frac{1}{2} P(q_{il})^{-1} \mid P(q_{il}) A(q_{il}) \mid \Delta_{il} q \qquad (25)$$

where P is the preconditioning matrix. With respect to the original Roe scheme, only the dissipative terms are altered and therefore the numerical scheme remains a consistant approximation of the time dependent compressible Euler equations. In this work, we use the preconditioner proposed by Turkel in [5]. In term of the "primitive" variables $U = [p,\, u,\, v,\, ln(p/(\rho^\gamma))]$, this preconditioner writes :

$$P = \begin{pmatrix} \beta^2 & 0 & 0 & 0 \\ 0 & 1 & 0 & 0 \\ 0 & 0 & 1 & 0 \\ 0 & 0 & 0 & 1 \end{pmatrix}$$

where β is a small factor of the order of the Mach number. For the conservative variables $q = [\rho, \rho u, \rho v, \rho e]$ the corresponding form is :

$$P(q) = \frac{\partial q}{\partial U}\, P(U)\, \frac{\partial U}{\partial q}$$

To obtain an explicit expression for the stabilization term :

$$P(q_{il})^{-1} \mid P(q_{il})\, A(q_{il}) \mid \Delta_{il}\, q$$

close to the expression obtained for the original scheme, we first diagonalize the matrix $P(q_{il})\, A(q_{il})$. Its eigenvalues $\lambda_k(q_{il})$ are given by :

$$\begin{aligned} \lambda_1 &= U_{il}, \\ \lambda_2 &= U_{il}, \\ \lambda_3 &= \frac{1}{2}\left((1+\beta^2)\, U_{il} + \sqrt{X}\right), \\ \lambda_4 &= \frac{1}{2}\left((1+\beta^2)\, U_{il} - \sqrt{X}\right). \end{aligned} \tag{26}$$

with $X = [(1-\beta^2)\, U_{il}]^2 + 4\,\beta^2\, a_{il}^2$. The product of the eigenvectors of $P(q_{il})\, A(q_{il})$ by $P(q_{il})^{-1}$ results in expressions that are close to the expressions of the eigenvectors of the Roe's matrix (see equations (41) of appendix I) :

$$\begin{aligned} R_1(q_{il}) &= \begin{bmatrix} 1 \\ u_{il} \\ v_{il} \\ \dfrac{u_{il}^2 + v_{il}^2}{2} \end{bmatrix}, \qquad R_2(q_{il}) = \begin{bmatrix} 0 \\ -(n_y)_{il} \\ (n_x)_{il} \\ V_{il} \end{bmatrix}, \\ R_3(q_{il}) &= \begin{bmatrix} 1 \\ u_{il} + r\,(n_x)_{il} \\ v_{il} + r\,(n_y)_{il} \\ h_{il} + r\, U_{il} \end{bmatrix}, \quad R_4(q_{il}) = \begin{bmatrix} 1 \\ u_{il} + s\,(n_x)_{il} \\ v_{il} + s\,(n_y)_{il} \\ h_{il} + s\, U_{il} \end{bmatrix}, \end{aligned} \tag{27}$$

where $r = \lambda_3 - U_{il}\,\beta^2$ and $s = \lambda_4 - U_{il}\,\beta^2$.

If we now, introduce the coordinate $\alpha_k(\Delta_{il}q)$ of the jump $\Delta_{il}q$ in the basis of the eigenvectors of $P(q_{il})\,A(q_{il})$ whose expressions are :

$$\begin{aligned}
\alpha_1(\Delta_{il}q) &= \Delta_{il}\rho - \frac{\Delta_{il}p}{a_{il}^2}, \\
\alpha_2(\Delta_{il}q) &= \rho_{il}\,\Delta_{il}V, \\
\alpha_3(\Delta_{il}q) &= \frac{1}{\sqrt{X}}\left(\frac{\Delta_{il}p}{r} + \rho_{il}\,\Delta_{il}U\right), \\
\alpha_4(\Delta_{il}q) &= \frac{1}{\sqrt{X}}\left(\frac{\Delta_{il}p}{-s} - \rho_{il}\,\Delta_{il}U\right).
\end{aligned} \tag{28}$$

we get :

$$P(q_{il})^{-1} \mid P(q_{il})A(q_{il}) \mid \Delta_{il}q = \sum_{k=1}^{4} \alpha_k(\Delta_{il}) \mid \lambda_k(q_{il}) \mid R_k(q_{il}).$$

or in developped form :

$$P(q_{il})^{-1} \mid P(q_{il})A(q_{il}) \mid \Delta_{il}q =$$

$$\begin{bmatrix}
\mid U_{il} \mid \alpha_1(\Delta_{il}q) & & +d_2\,\dfrac{\Delta_{il}p}{a_{il}^2} & +d_1\rho_{il}\Delta_{il}U \\
\mid U_{il} \mid \alpha_1(\Delta_{il}q)\,u_{il} & -\rho_{il} \mid U_{il} \mid (n_y)_{il}\,\Delta_{il}V & +d_4\,\dfrac{\Delta_{il}p}{a_{il}^2} & +d_3\,\rho_{il}\,\Delta_{il}U \\
\mid U_{il} \mid \alpha_1(\Delta_{il}q)\,v_{il} & +\rho_{il} \mid U_{il} \mid (n_x)_{il}\,\Delta_{il}V & +d_6\,\dfrac{\Delta_{il}p}{a_{il}^2} & +d_5\,\rho_{il}\,\Delta_{il}U \\
\mid U_{il} \mid \alpha_1(\Delta_{il}q)\,\dfrac{u_{il}^2 + v_{il}^2}{2} & +\rho_{il} \mid U_{il} \mid V_{il}\,\Delta_{il}V & +d_8\,\dfrac{\Delta_{il}p}{a_{il}^2} & +d_7\,\rho_{il}\,\Delta_{il}U
\end{bmatrix} \tag{29}$$

where

$$d_1 = \frac{U_{il}}{\sqrt{X}}\,\left(1+\beta^2\right), \quad d_2 = \frac{U_{il}^2}{\sqrt{X}}\,\left(\beta^2 - 1 + \frac{2\,a_{il}^2}{U_{il}^2}\right), \tag{30}$$

and

$$
\begin{aligned}
d_3 &= u_{\boldsymbol{il}}\, d_1 + (n_x)_{\boldsymbol{il}}\, d_9, & d_4 &= u_{\boldsymbol{il}}\, d_2 - s\, r\, (n_x)_{\boldsymbol{il}}\, d_1/\beta^2, \\
d_5 &= v_{\boldsymbol{il}}\, d_1 + (n_y)_{\boldsymbol{il}}\, d_9, & d_6 &= v_{\boldsymbol{il}}\, d_2 - s\, r\, (n_y)_{\boldsymbol{il}}\, d_1/\beta^2, \\
d_7 &= h_{\boldsymbol{il}}\, d_1 + U_{\boldsymbol{il}}\, d_9, & d_8 &= h_{\boldsymbol{il}}\, d_2 - s\, r\, U_{\boldsymbol{il}}\, d_1/\beta^2, \\
d_9 &= \frac{U_{\boldsymbol{il}}^2}{\sqrt{X}} \left(1 - \beta^2 + \frac{2\,\beta^2\, a_{\boldsymbol{il}}^2}{U_{\boldsymbol{il}}^2}\right).
\end{aligned}
\tag{31}
$$

and we have used $\mid \lambda_3 \mid = \lambda_3$ and $\mid \lambda_4 \mid = -\lambda_4$ because for low Mach number, one can easily check that $\lambda_3 > 0$ and $\lambda_4 < 0$.

Now, using the same dimensionless variables as in the previous cases, we write the resulting scheme in non-dimensionalized form. For this, we need to non-dimensionalize the parameter β that appears in the preconditioner. Since in practice, this parameter is chosen of the order of the Mach number, we take :

$$\beta = M_* \tilde{\beta}$$

and $\tilde{\beta}$ is a parameter of order unity. In practice, β is often chosen constant in the whole computational domain, here we consider the more general case where this quantity can be allowed to become a function of the local variables. We also note that the variable $X = [(1-\beta^2)\, U_{\boldsymbol{il}}]^2 + 4\,\beta^2\, a_{\boldsymbol{il}}^2$ can be evaluated as :

$$X = u_*^2 [\tilde{U}_{\boldsymbol{il}}^2 (1-\tilde{\beta}^2)^2 + 4\tilde{\beta}^2 \tilde{a}_{\boldsymbol{il}}^2]$$

and we introduce for convenience the notation $Y = \tilde{U}_{\boldsymbol{il}}^2 (1-\tilde{\beta}^2)^2 + 4\tilde{\beta}^2 \tilde{a}_{\boldsymbol{il}}^2$ where Y is a variable of order unity; Once again, in the equations below, we dropped the symbol $\tilde{}$ to simplify the notations. We then obtain :

$$\frac{1}{2M_*^2}\sum_{l\in\mathcal{V}(i)}\frac{2\Delta_{il}p}{\sqrt{Y_{il}}}+$$
$$\tilde{\delta}\frac{d}{dt}\rho_i+\frac{1}{2}\sum_{l\in\mathcal{V}(i)}\rho_l\vec{u}_l.\vec{n}_{il}+|U_{il}|(\Delta_{il}\rho-\frac{\Delta_{il}p}{a_{il}^2})-\frac{U_{il}^2}{a_{il}^2}\frac{\Delta_{il}p}{\sqrt{Y_{il}}}+\rho_{il}\frac{U_{il}}{\sqrt{Y_{il}}}\Delta_{il}U+$$
$$\frac{M_*^2}{2}\sum_{l\in\mathcal{V}(i)}\beta^2(\rho_{il}\frac{U_{il}}{\sqrt{Y_{il}}}\Delta_{il}U+\frac{U_{il}^2}{a_{il}^2}\frac{\Delta_{il}p}{\sqrt{Y_{il}}})=0 \tag{32.a}$$

$$\frac{1}{2M_*^2}\sum_{l\in\mathcal{V}(i)}p_l(n_x)_{il}+\frac{(Un_x+2u)_{il}}{\sqrt{Y_{il}}}\Delta_{il}p+$$

$$\tilde{\delta}\frac{d}{dt}\rho_i u_i+\frac{1}{2}\sum_{l\in\mathcal{V}(i)}\rho_l u_l\vec{u}_l.\vec{n}_{il}+|U_{il}|(\Delta_{il}\rho-\frac{\Delta_{il}p}{a_{il}^2})u_{il}-\rho_{il}|U_{il}|(n_y)_{il}\Delta_{il}V+$$
$$\frac{(u+Un_x)_{il}U_{il}+2\beta^2a_{il}^2}{\sqrt{Y_{il}}}\rho_{il}\Delta_{il}U+\frac{\beta^2a_{il}^2U_{il}(n_x)_{il}-u_{il}U_{il}^2}{\sqrt{Y_{il}}}\frac{\Delta_{il}p}{a_{il}^2}+$$

$$\frac{M_*^2}{2}\sum_{l\in\mathcal{V}(i)}\beta^2[\frac{(u-Un_x)_{il}U_{il}}{\sqrt{Y_{il}}}\rho_{il}\Delta_{il}U+\frac{u_{il}U_{il}^2}{\sqrt{Y_{il}}}\frac{\Delta_{il}p}{a_{il}^2}]=0 \tag{32.b}$$

$$\frac{1}{2M_*^2}\sum_{l\in\mathcal{V}(i)}p_l(n_y)_{il}+\frac{(Un_y+2v)_{il}}{\sqrt{Y_{il}}}\Delta_{il}p+$$

$$\tilde{\delta}\frac{d}{dt}\rho_i v_i+\frac{1}{2}\sum_{l\in\mathcal{V}(i)}\rho_l v_l\vec{u}_l.\vec{n}_{il}+|U_{il}|(\Delta_{il}\rho-\frac{\Delta_{il}p}{a_{il}^2})v_{il}+\rho_{il}|U_{il}|(n_x)_{il}\Delta_{il}V+$$
$$\frac{(v+Un_y)_{il}U_{il}+2\beta^2a_{il}^2}{\sqrt{Y_{il}}}\rho_{il}\Delta_{il}U+\frac{\beta^2a_{il}^2U_{il}(n_y)_{il}-v_{il}U_{il}^2}{\sqrt{Y_{il}}}\frac{\Delta_{il}p}{a_{il}^2}+$$

$$\frac{M_*^2}{2}\sum_{l\in\mathcal{V}(i)}\beta^2[\frac{(v-Un_y)_{il}U_{il}}{\sqrt{Y_{il}}}\rho_{il}\Delta_{il}U+\frac{v_{il}U_{il}^2}{\sqrt{Y_{il}}}\frac{\Delta_{il}p}{a_{il}^2}]=0 \tag{32.c}$$

$$\frac{1}{2M_*^2}\sum_{l\in\mathcal{V}(i)}\frac{2h_{il}}{\sqrt{Y_{il}}}\Delta_{il}p+$$
$$\tilde{\delta}\frac{d}{dt}\rho_i e_i+\frac{1}{2}\sum_{l\in\mathcal{V}(i)}(\rho_l e_l+p_l)\vec{u}_l.\vec{n}_{il}+\frac{(h_{il}+a_{il}^2)}{\sqrt{Y_{il}}}U_{il}^2\frac{\Delta_{il}p}{a_{il}^2}+\frac{h_{il}}{\sqrt{Y_{il}}}U_{il}\rho_{il}\Delta_{il}U+$$
$$\frac{M_*^2}{2}\sum_{l\in\mathcal{V}(i)}|U_{il}|(\Delta_{il}\rho-\frac{\Delta_{il}p}{a_{il}^2})(\frac{u_{il}^2+v_{il}^2}{2})+\rho_{il}|U_{il}|V_{il}\Delta_{il}V+\beta^2\frac{(h_{il}+a_{il}^2)U_{il}^2}{\sqrt{Y_{il}}}\frac{\Delta_{il}p}{a_{il}^2}+$$
$$\frac{U_{il}^3+\beta^2(h_{il}+2a_{il}^2)U_{il}}{\sqrt{Y_{il}}}\rho_{il}\Delta_{il}U-\frac{M_*^4}{2}\sum_{l\in\mathcal{V}(i)}\beta^2U_{il}^3\rho_{il}\Delta_{il}U=0 \tag{32.d}$$

Comparing this system with the analogous one (15) obtained in the case with no preconditioning, we note that now, dissipation terms of order $1/M_*^2$ appear in the continuity and energy equations and that all the dissipative terms of order $1/M_*$ have disappeared. This will force the pressure fluctuations to be smaller than in the case with no preconditioning. To see that, we expand now the variables in power of the reference Mach number and introduce these expansions in the equations (32). We obtain at order $1/M_*^2$:

1. Continuity equation

$$\sum_{l\in\mathcal{V}(i)} \frac{\Delta_{il} p^0}{\sqrt{Y^0_{il}}} = 0 \tag{33}$$

2. horizontal momentum equation

$$\sum_{l\in\mathcal{V}(i)} p^0_l (n_x)_{il} + \frac{(U^0 n_x + 2u^0)_{il}}{\sqrt{Y^0_{il}}} \Delta_{il} p^0 = 0 \tag{34}$$

3. vertical momentum equation

$$\sum_{l\in\mathcal{V}(i)} p^0_l (n_y)_{il} + \frac{(U^0 n_y + 2v^0)_{il}}{\sqrt{Y^0_{il}}} \Delta_{il} p^0 = 0 \tag{35}$$

4. energy equation

$$\sum_{l\in\mathcal{V}(i)} \frac{2h^0_{il}}{\sqrt{Y^0_{il}}} \Delta_{il} p^0 = 0 \tag{36}$$

with $Y^0 = (U^0_{il})^2 + 4\beta^2 (a^0_{il})^2$. Let us look for the solutions of (33) (34)- (35)- (36). This is a system of four homogeneous "elliptic" difference equations for the N values of the 0-order pressure p^0 at the interior points of the computational domain. Obviously, $p^0 \equiv$ constant is a common solution of these 4 equations. However, depending on the boundary conditions, these equations may also have non-constant solutions and the problem is to establish that the intersection of the kernels of these 4 equations is reduced to constant vectors. For general arbitrary boundary conditions, we have not been able to prove this result. However, we give below two important cases where this result can be established.
First, we remark that in (33) and (36), the coefficients are positive, therefore the discrete maximum applies and an interior point cannot be an extremum. Therefore, the extrema of the pressure field are on the boundary. This implies that if the pressure is constant on the

boundary of the computational domain, then it is constant everywhere in the domain.

We now proceed to show the same result if the density is constant on the boundary of the computational domain. Assume that the p^0 pressure is not constant and denote $\boldsymbol{i}$ the point where the maximum value of the pressure is attained (this point always exists because there is a finite number of computational nodes). Because the maximum principle applies, this point is a neighbor of a boundary node. To fix the idea, assume that this boundary is the left one (see figure 4). Because, the pressure in $\boldsymbol{i}$ is maximum, the differences $\Delta_{\boldsymbol{il}} p^0$ for $\boldsymbol{l} \in \{N, S, E\}$ are positive and this implies that $p^0(A) > p^0_{\boldsymbol{i}}$ (this is indicated by a "$>$" symbol on figure 4). Now consider equation (33) (or (36)) written at nodes E for instance, because $p^0_{\boldsymbol{i}} > p^0(E)$ there must be at least one neighor of E whose pressure is less than the pressure in E. Repeating the argument for this node, we see that we can construct a path $\mathcal{P} = \{A, \boldsymbol{i}, E, \ldots, \boldsymbol{k}, \boldsymbol{k}+1, \ldots\}$ such that for any $\boldsymbol{k}$ in this list $p^0_{\boldsymbol{k}} > p^0_{\boldsymbol{k}+1}$. Since this path cannot make closed loops, it necessarily ends on the boundary. Let us call B the point of the boundary where it ends. Obviously we have $p^0(A) > p^0(B)$.

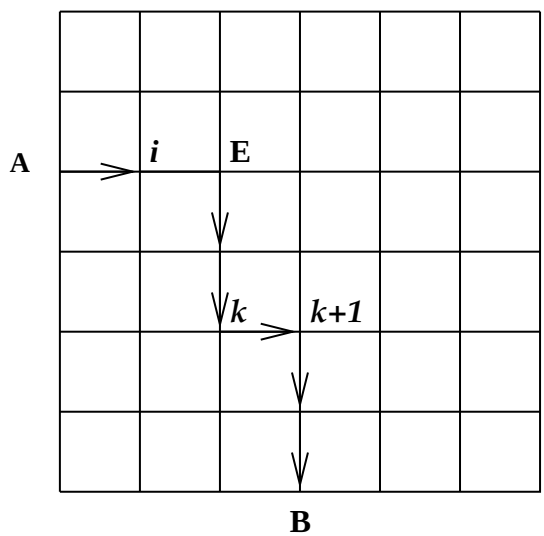

Figure 4: Path connecting points with decreasing pressures

We remark now that for any interior point, we can rewrite the system (33) (34)- (35)- (36) in the form of a system of four equations for the four unknowns $\Delta_{\boldsymbol{il}} p^0$. Since the coefficients of the three equations (33) (34)- (35) are obviously different and arbitrary (they depend on the velocity field), the only possible way for this system to have a non-zero solution is that equation (36) is proportional to equation (33). This implies that the four values $h^0_{\boldsymbol{il}}$ are

equal. Since $h^0_{\boldsymbol{il}}$ is an average of the value of h^0 in $\boldsymbol{i}$ and $\boldsymbol{l}$ we make the reasonable assumption that this implies that the four values $h^0_{\boldsymbol{l}}$ are equal. Now, considering again the path $\mathcal{P}$ we see that this implies that the specific entalpy h^0 is constant along this path. But it is easily checked from the $0-th$ order state law that the $0-th$ specific entalpy h^0 is defined by $h^0 = \dfrac{\gamma p^0}{(\gamma-1)\rho^0}$. Thus if $p^0(A) > p^0(B)$, $h^0(A) = h^0(B)$ implies that $\rho^0(A) > \rho^0(B)$ but this is impossible since we have assumed that the density is constant on the boundary.

We also remark from the previous proof, that if the temperature field is not constant in the computational domain, then the $h^0_{\boldsymbol{il}}$ will be different and then the argument given above shows that the p^0 pressure field is constant. We collect these results in :

Lemma 4.1 *Assume either that :*

i) The $0-$ *order temperature field* T^0 *is not constant*

ii) The $0-$ *order pressure* p^0 *is constant on the boundary*

iii) The $0-$ *order density* ρ^0 *is constant on the boundary*

then the $1/M_*^2$ *equations (33) (34)- (35)- (36) imply that* $p^0_{\boldsymbol{l}} = cte\ \forall \boldsymbol{l}$.

Since there are no $1/M_*$ term in the equations (32), the order $1/M_*$ equations that result from the expansion (16) are totally identical to the order $1/M_*^2$ equations with p^0 replaced by p^1. Therefore the same argument as for the order 0 pressure can be used and we have :

Proposition 4.1 *Under the assumptions of lemma 4.1, the solutions of the discrete equations with preconditioned dissipation support pressure fluctuations of order* M_*^2 *:*

$$p(x,t) = P_0(t) + M_*^2 p_2(x,t) \tag{37}$$

Remark : Comparing the case of the preconditioned dissipation with the one of the original Roe scheme, we note that in this latter case, the $1/M_*$ equations link the pressure differences with the velocity differences. A consequence is that the order M_* pressure p^1 *cannot* be constant. On the other hand, for the preconditioned dissipation, the order $1/M_*^2$ and $1/M_*$ equations involved only the pressure differences. The possibility to get a non-constant pressure in this case is related to the fact that the kernels of the difference equations may contain non constant vectors. This is a well known problem for the approximation of the incompressible equations on collocated meshes that do not satisfy the inf-sup criterion. In some sense the appearance of this type of problem was not unexpected.

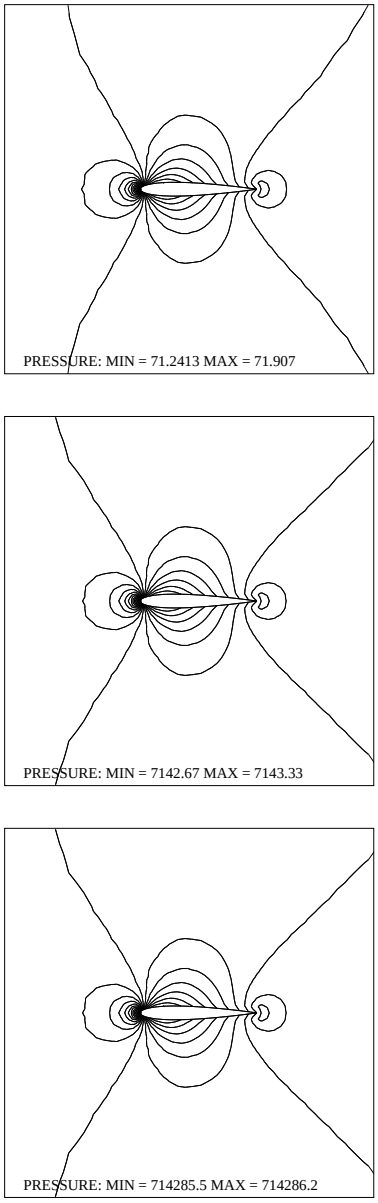

Figure 5: Isovalues of the pressure, on a 3114 node mesh for $M_\infty = 0.1$ (top), $M_\infty = 0.01$ (middle), $M_\infty = 0.001$ (bottom). Preconditioned dissipation.

To conclude this section, we return to the numerical experiments performed in section 3. Figure 5 presents the pressure fields for the same three decreasing inflow Mach number as in Figure 2 on the same fixed mesh. In contrast to the results obtained with the original Roe scheme, we note now that the solutions converge to a unique solution (Actually, the isovalues for these three Mach numbers are almost undistinguishable). Figure 6 presents the pressure fluctuations with respect to the Mach number. As in the previous section, the agreement with the theory is remarkable : the pressure fluctuations scale exactly with the square of the Mach number as in the continuous case.

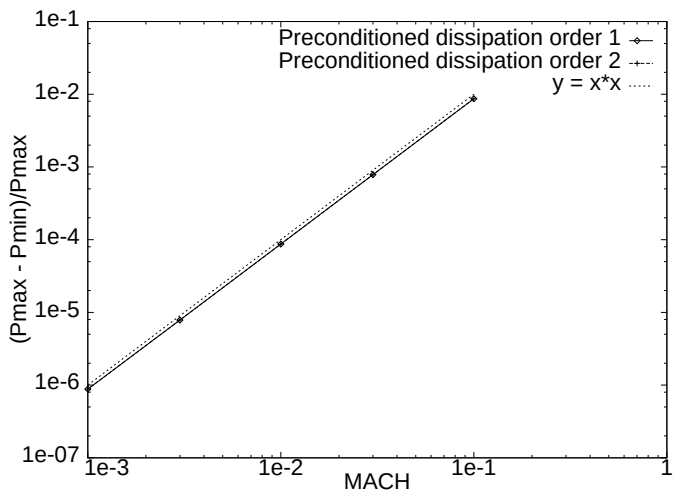

Figure 6: Pressure fluctuations versus inflow Mach number; solid line : order 1, dashed line : order 2. For comparison, the curve $y = x^2$ is represented by a dotted line.

5 Conclusion

Using an asymptotic analysis of the discrete upwind approximation of the compressible Euler equations, we provide a detailed explanation of the mechanism that produces the failure of compressible code to compute very subsonic flows. We show rigourously that in the low Mach number limit, the discrete equations support pressure fluctuations of the order of the Mach number while in the solutions of the continuous equations, the pressure scales with the *square* of the Mach number. The theory is totally confirmed by numerical experiments. We next examine the case where the numerical dissipation is altered with the help of the preconditioning matrix proposed in [5]. For this latter case, we show that the solution of the discrete equations possesses pressure fluctuations of the correct magnitude. Again, numerical experiments confirm the theoretical results.

6 Acknowledgments

We are grateful to Dr A. Dervieux for fruitful discussions we had. We also thank Dr E. Turkel for information he gave us on his experience on preconditioning methods. This report is part of the second author's thesis work which has been jointly supported by CNES and RENAULT.

Appendix I. Roe's approximate Riemann solver

Let us write the 2-D compressible Euler equations (3) in the conservative form :

$$\frac{\partial q}{\partial t} + \nabla \cdot \vec{F}(q) = 0, \qquad \vec{F}(q) = \begin{pmatrix} F_1(q) \\ F_2(q) \end{pmatrix}, \tag{38}$$

where

$$q = \begin{bmatrix} \rho \\ \rho\, u \\ \rho\, v \\ \rho\, e \end{bmatrix}, \; F_1(q) = \begin{bmatrix} \rho\, u \\ \rho\, u^2 + p \\ \rho\, u\, v \\ (\rho\, e + p)\, u \end{bmatrix}, \; F_2(q) = \begin{bmatrix} \rho\, v \\ \rho\, u\, v \\ \rho\, v^2 + p \\ (\rho\, e + p)\, v \end{bmatrix}. \tag{39}$$

Integrating these equations on a control volume $C_{\boldsymbol{i}}$ we get :

$$\delta^2 \frac{dq_{\boldsymbol{i}}}{dt} + \sum_{\boldsymbol{l} \in \mathcal{V}(\boldsymbol{i})} \delta\, \Phi(q_{\boldsymbol{i}}, q_{\boldsymbol{l}}, \vec{n}_{\boldsymbol{il}}) = 0. \tag{40}$$

where $\Phi(q_{\boldsymbol{i}}, q_{\boldsymbol{l}}, \vec{n}_{\boldsymbol{il}})$, the numerical flux function approximates $\frac{1}{\delta} \int_{\partial C_{\boldsymbol{i}} \cap \partial C_{\boldsymbol{l}}} \vec{F}.\vec{n} dl$. For Roe scheme, this function is defined by :

$$\Phi(q_{\boldsymbol{i}}, q_{\boldsymbol{l}}, \vec{n}_{\boldsymbol{il}}) = \frac{\vec{F}(q_{\boldsymbol{i}}) + \vec{F}(q_{\boldsymbol{l}})}{2} \cdot \vec{n_{\boldsymbol{il}}} + \frac{1}{2} \mid A(q_{\boldsymbol{il}}, \vec{n_{\boldsymbol{il}}}) \mid \Delta_{\boldsymbol{il}} q,$$

where the matrix $A(q_{\boldsymbol{il}}, \vec{n_{\boldsymbol{il}}})$ satisfies the following property:

$$A(q_{\boldsymbol{il}}, \vec{n_{\boldsymbol{il}}})\, \Delta_{\boldsymbol{il}} q = (\vec{F}(q_{\boldsymbol{i}}) - \vec{F}(q_{\boldsymbol{l}})) \cdot \vec{n_{\boldsymbol{il}}}$$

If we introduce the eigenvectors of matrix $A(q_{\boldsymbol{il}}, \vec{n_{\boldsymbol{il}}})$:

$$R_1(q_{\boldsymbol{il}}) = \begin{bmatrix} 1 \\ u_{\boldsymbol{il}} \\ v_{\boldsymbol{il}} \\ \dfrac{u_{\boldsymbol{il}}^2 + v_{\boldsymbol{il}}^2}{2} \end{bmatrix}, \qquad R_2(q_{\boldsymbol{il}}) = \begin{bmatrix} 0 \\ -(n_y)_{\boldsymbol{il}} \\ (n_x)_{\boldsymbol{il}} \\ V_{\boldsymbol{il}} \end{bmatrix},$$
$$R_3(q_{\boldsymbol{il}}) = \begin{bmatrix} 1 \\ u_{\boldsymbol{il}} + a_{\boldsymbol{il}}\, (n_x)_{\boldsymbol{il}} \\ v_{\boldsymbol{il}} + a_{\boldsymbol{il}}\, (n_y)_{\boldsymbol{il}} \\ h_{\boldsymbol{il}} + a_{\boldsymbol{il}}\, U_{\boldsymbol{il}} \end{bmatrix}, \quad R_4(q_{\boldsymbol{il}}) = \begin{bmatrix} 1 \\ u_{\boldsymbol{il}} - a_{\boldsymbol{il}}\, (n_x)_{\boldsymbol{il}} \\ v_{\boldsymbol{il}} - a_{\boldsymbol{il}}\, (n_y)_{\boldsymbol{il}} \\ h_{\boldsymbol{il}} - a_{\boldsymbol{il}}\, U_{\boldsymbol{il}} \end{bmatrix}, \tag{41}$$

where

$$U_{il} = u_{il}\,(n_x)_{il} + v_{il}\,(n_y)_{il},$$
$$V_{il} = -u_{il}\,(n_y)_{il} + v_{il}\,(n_x)_{il}.$$

these eigenvectors form a complete base of $I\!R^4$ and any vector $X = (X_1, X_2, X_3, X_4)^t$ can be written as :

$$X = \sum_{k=1}^{4} \alpha_k(X) R_k$$

where the coordinates α_k in this base are defined by :

$$\begin{aligned} \alpha_1 &= X_1 - \frac{\mathcal{E}}{a_{il}^2}, & \alpha_2 &= \mathcal{B} \\ \alpha_3 &= \frac{1}{2}\left(\frac{\mathcal{E}}{a_{il}^2} + \frac{\mathcal{A}}{a_{il}}\right), & \alpha_4 &= \frac{1}{2}\left(\frac{\mathcal{E}}{a_{il}^2} - \frac{\mathcal{A}}{a_{il}}\right) \end{aligned} \tag{42}$$

with

$$\begin{aligned} \mathcal{E} &= (\gamma-1)(X_4 - v_{il} X_3 - u_{il} X_2 + \frac{u_{il}^2 + v_{il}^2}{2} X_1), \\ \mathcal{A} &= (n_x)_{il}\, X_2 + (n_y)_{il}\, X_3 - U_{il}\, X_1 \\ \mathcal{B} &= -(n_y)_{il}\, X_2 + (n_x)_{il}\, X_3 - V_{il}\, X_1 \end{aligned} \tag{43}$$

As remarked by Abgrall in [2], for any $D \neq 0$ the Δ_{il} operator obeys the following rules :

$$\Delta_{il}(ab) = \underline{a}\Delta_{il} b + \bar{b}\Delta_{il} a$$

with

$$\underline{a} = \frac{a_i + D a_l}{1+D}, \quad \bar{a} = \frac{a_l + D a_i}{1+D}$$

Moreover if $D = \sqrt{\rho_i}/\sqrt{\rho_l}$, we have the additional property :

$$\underline{\rho a} = \underline{\rho}\bar{a} \tag{44}$$

This simplify to some extend the expression of the numerical dissipation since we obtain :

$$\begin{aligned} \alpha_1(\Delta_{il} q) &= \Delta_{il}\rho - \frac{\Delta_{il} p}{a_{il}^2}, \\ \alpha_2(\Delta_{il} q) &= \rho_{il}\, \Delta_{il} V, \\ \alpha_3(\Delta_{il} q) &= \frac{1}{2\, a_{il}}\left(\frac{\Delta_{il} p}{a_{il}} + \rho_{il}\, \Delta_{il} U\right), \\ \alpha_4(\Delta_{il} q) &= \frac{1}{2\, a_{il}}\left(\frac{\Delta_{il} p}{a_{il}} - \rho_{il}\, \Delta_{il} U\right). \end{aligned} \tag{45}$$

Writing the numerical dissipation under the form :

$$\mid A(q_{\boldsymbol{il}}, \vec{n}_{\boldsymbol{il}}) \mid \ \Delta_{\boldsymbol{il}} q = \sum_{k=1}^{4} \alpha_k(\Delta_{\boldsymbol{il}} q) \ \mid \lambda_k(q_{\boldsymbol{il}}) \mid R_k(q_{\boldsymbol{il}}). \tag{46}$$

with the eigenvalue $\lambda_k(q_{\boldsymbol{il}})$ given by :

$$\begin{array}{rclrcl} \lambda_1 & = & U_{\boldsymbol{il}}, & \lambda_2 & = & U_{\boldsymbol{il}}, \\ \lambda_3 & = & U_{\boldsymbol{il}} + a_{\boldsymbol{il}}, & \lambda_4 & = & U_{\boldsymbol{il}} - a_{\boldsymbol{il}}, \end{array} \tag{47}$$

we then obtain :

$$\mid A(q_{\boldsymbol{il}}) \mid \ \Delta_{\boldsymbol{il}} q =$$

$$\left[\begin{array}{llll} \mid U_{\boldsymbol{il}} \mid \ \alpha_1(\Delta_{\boldsymbol{il}} q) & & +d_2 \dfrac{\Delta_{\boldsymbol{il}} p}{a_{\boldsymbol{il}}^2} & +d_1 \rho_{\boldsymbol{il}} \Delta_{\boldsymbol{il}} U \\ \mid U_{\boldsymbol{il}} \mid \ \alpha_1(\Delta_{\boldsymbol{il}} q)\, u_{il} & -\rho_{\boldsymbol{il}} \mid U_{\boldsymbol{il}} \mid (n_y)_{\boldsymbol{il}} \Delta_{\boldsymbol{il}} V & +d_4 \dfrac{\Delta_{\boldsymbol{il}} p}{a_{\boldsymbol{il}}^2} & +d_3 \rho_{\boldsymbol{il}} \Delta_{\boldsymbol{il}} U \\ \mid U_{\boldsymbol{il}} \mid \ \alpha_1(\Delta_{\boldsymbol{il}} q)\, v_{il} & +\rho_{\boldsymbol{il}} \mid U_{\boldsymbol{il}} \mid (n_x)_{\boldsymbol{il}} \Delta_{\boldsymbol{il}} V & +d_6 \dfrac{\Delta_{\boldsymbol{il}} p}{a_{\boldsymbol{il}}^2} & +d_5 \rho_{\boldsymbol{il}} \Delta_{\boldsymbol{il}} U \\ \mid U_{\boldsymbol{il}} \mid \ \alpha_1(\Delta_{\boldsymbol{il}} q) \dfrac{u_{il}^2 + v_{il}^2}{2} & +\rho_{\boldsymbol{il}} \mid U_{\boldsymbol{il}} \mid V_{\boldsymbol{il}} \Delta_{\boldsymbol{il}} V & +d_8 \dfrac{\Delta_{\boldsymbol{il}} p}{a_{\boldsymbol{il}}^2} & +d_7 \rho_{\boldsymbol{il}} \Delta_{\boldsymbol{il}} U \end{array} \right] \tag{48}$$

with

$$\begin{array}{ll} d_1 = \dfrac{U_{\boldsymbol{il}}}{a_{\boldsymbol{il}}} & d_2 = a_{\boldsymbol{il}} \\ d_3 = \dfrac{U_{\boldsymbol{il}}}{a_{\boldsymbol{il}}} u_{\boldsymbol{il}} + a_{\boldsymbol{il}} (n_x)_{\boldsymbol{il}} & d_4 = a_{\boldsymbol{il}} (U n_x + u)_{\boldsymbol{il}} \\ d_5 = \dfrac{U_{\boldsymbol{il}}}{a_{\boldsymbol{il}}} v_{\boldsymbol{il}} + a_{\boldsymbol{il}} (n_y)_{\boldsymbol{il}} & d_6 = a_{\boldsymbol{il}} (U n_y + v)_{\boldsymbol{il}} \\ d_7 = U_{\boldsymbol{il}} (\dfrac{h_{\boldsymbol{il}}}{a_{\boldsymbol{il}}} + a_{\boldsymbol{il}}) & d_8 = a_{\boldsymbol{il}} (h + U^2)_{\boldsymbol{il}} \end{array} \tag{49}$$

References

[1] Klainerman S. Majda A. Compressible and incompressible fluids. *Comm. Pure Appl. Math*, 35:629–653, 1982.

[2] Rémi Abgrall. An extension of Roe's upwind scheme to algebraic equilibrium real gas models. *Computers and Fluids*, 19(2):171–182, 1991.

[3] Y.-H. Choi and C. L. Merkle. The application of preconditioning in viscous flows. *J. Comp. Phys.*, 105:207 – 223, 1993.

[4] A. G. Godfrey, R. W. Walters, and B. van Leer. Preconditioning for the Navier-Stokes equations with finite-rate chemistry. *AIAA Paper 93-0535*, 1993.

[5] E. Turkel. Preconditioned methods for solving the incompressible and low speed compressible equations. *J. Comp. Phys.*, 72:277 – 298, 1987.

[6] E. Turkel. Review of preconditioning methods for fluid dynamics. *Applied Numerical Mathematics*, 12:257 – 284, 1993.

[7] E. Turkel, A. Fiterman, and B. van Leer. Preconditioning and the limit to the incompressible flow equations. Technical Report 93-42, ICASE, 1993.

[8] C. Viozat. Implicit upwind schemes for low Mach number compressible flows. Technical Report 3084, INRIA, 1997.

[9] G. Volpe. Performance of compressible flow codes at low Mach number. *AIAA Journal*, 31(1):49–56, 93.

Unité de recherche INRIA Lorraine, Technopôle de Nancy-Brabois, Campus scientifique,
615 rue du Jardin Botanique, BP 101, 54600 VILLERS LÈS NANCY
Unité de recherche INRIA Rennes, Irisa, Campus universitaire de Beaulieu, 35042 RENNES Cedex
Unité de recherche INRIA Rhône-Alpes, 655, avenue de l'Europe, 38330 MONTBONNOT ST MARTIN
Unité de recherche INRIA Rocquencourt, Domaine de Voluceau, Rocquencourt, BP 105, 78153 LE CHESNAY Cedex
Unité de recherche INRIA Sophia Antipolis, 2004 route des Lucioles, BP 93, 06902 SOPHIA ANTIPOLIS Cedex

Éditeur
INRIA, Domaine de Voluceau, Rocquencourt, BP 105, 78153 LE CHESNAY Cedex (France)
ISSN 0249-6399